Supplemental Data

Pericentric Chromatin Is Organized into an Intramolecular Loop in Mitosis

Elaine Yeh, Julian Haase, Leocadia V. Paliulis, Ajit Joglekar, Lisa Bond, David Bouck, E.D. Salmon, and Kerry Bloom

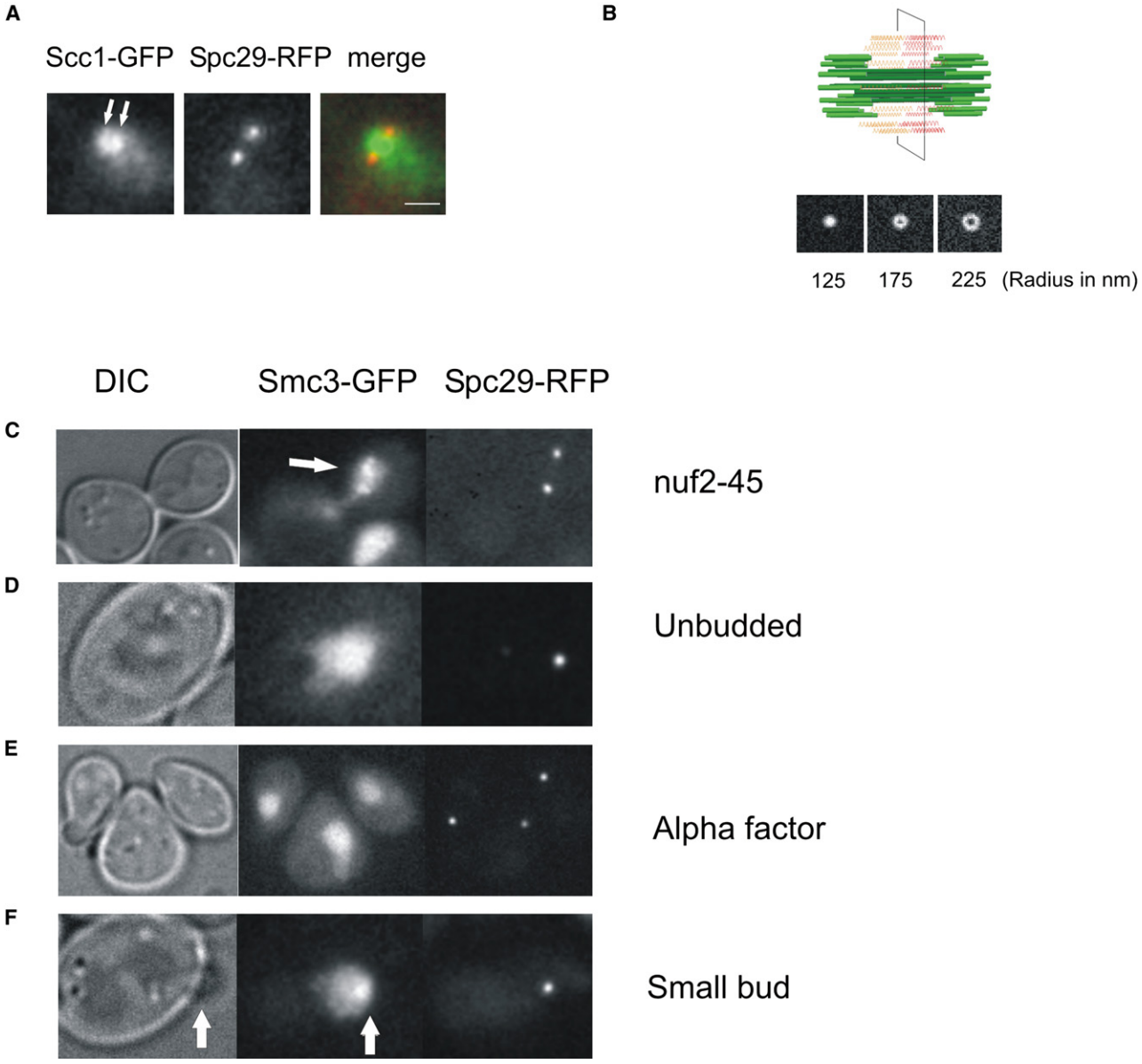

Figure S1. Cell-Cycle Regulation and Modeling of the Cohesin Cylinder

(A) Scc1-GFP is concentrated between the spindle-pole bodies in metaphase. Two oblongate lobes of Scc1-GFP fluorescence (arrows) lie between the spindle poles of the mitotic apparatus (Spc29-RFP) in the sagittal section (Scc1-GFP green in merge; Spc29-RFP red in merge). Spindle length = 1.2 μm. Scale bar represents = 1 μm.

(B) Top: Schematic of the yeast spindle. Four interpolar microtubules from each SPB (dark green) and 16 kinetochore microtubules (light green) are arranged cylindrically [S3]. Bottom: Simulations of 16 circularly arranged planar fluorophores of indicated radius (in nm), representing 16 strands of chromatin bound to cohesin. The view is a cross-section through the central spindle. As the radius of the array decreases, the ability to visualize the central core decreases. The simulation of a cylinder with radius 175 nm approximates the experimental image in cross-section (Figure 2B).

(C) Loss of the outer core kinetochore component (*nuf2-45*) disrupts Smc3-GFP cylinder. Smc3-GFP is visible as one or more spots often (arrow) but is not always closely associated with one spindle pole.

(D) Smc3-GFP is diffuse in the nucleus of unbudded cells.

(E) Smc3-GFP is diffuse in the nucleus of cells arrested in alpha factor.

(F) Smc3-GFP accumulates near the SPB in S phase cells (small budded). Spc29-RFP denotes the position of the spindle-pole bodies. Arrows mark the position of the bud and Smc3-GFP concentration, respectively.

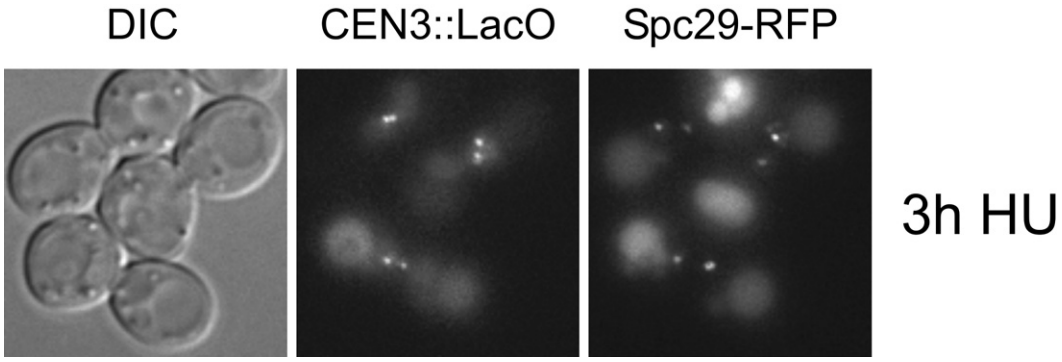

Figure S2. Centromere-DNA Replication in Hydroxyurea

Centromeres are replicated and separated in early S phase arrest by hydroxyurea (HU). Centromere proximal DNA was visualized with a LacO array integrated 3.8 kb from CEN3. Cells treated with 0.1M HU for 3 hr arrest as large budded cells. Centromere-DNA replication was observed in cells with two CEN3 LacO spots (CEN3::LacO, middle panel, visualized by LacI-GFP). Proper spindle assembly was determined by Spc29-RFP duplication and separation.

Supplemental Experimental Procedures

Yeast Strains and Media

The *S. cerevisiae* strains used for this study were as follows: for KBY1983, MATa, trp1Δ63, leu2Δ1, ura3-52, his3Δ200, lys2-801, SMC3-GFP::URA3 (pLF639), and SPC29-RFP-HYG; for KBY8022, MATa, trp1Δ63, leu2Δ1, ura3-52, his3Δ200, lys2-801, SMC3-GFP::URA3 (pLF639) SPC29-RFP-HYG, and NDC80-Cherry-Kan; for KBY1985, MATa, trp1Δ63, leu2Δ1, ura3-52, his3Δ200, lys2-801, SMC3-GFP::URA3(pLF639), and Tub3-CFP-KAN; for KBY8009, MATa, trp1Δ63, leu2Δ1, ura3-52, his3Δ200, lys2-801, SCC1-GFP-KAN, and SPC29-RFP:HYG; for KBY5114, MATa, leu2-3, 112, ura3-52, trp1Δ1, nuf2-45, SMC3-GFP::URA3 (pLF639), and SPC29-RFP:HYG; for DCB350.1, MATa, trp1Δ63, leu2Δ1, ura3-52, his3Δ200, lys2-801, HTB2-GFP-KAN, and SPC29-RFP-HYG; for KBY7006, MATa, trp1Δ63, leu2Δ1, ura3-52, his3Δ200, lys2-801, and Cse4-GFP-KAN; for KBY8901, MATa, ndc10-1::URA3, ndc10::TRP1, trp1Δ63, leu2Δ1, ura3-52, his3Δ200, lys2-801 SMC3-GFP::URA3 (pLF639), and SPC29-RFP:HYG; for DCB261.1, MATa, mcd1-1, leu2-3,112, ura3-52 and SPC29-RFP:HYG; and for KBY8039, MATa, ade2, his3, trp1, ura3-52, leu2-3,112, can1-100, LacINLSGFP:HIS3, lacO::URA3 (3.8 kb from CEN3), and SPC29-RFP-HYG. Plasmid pLF639 creates a single-copy GFP fusion at the SMC3 locus and was kindly provided by A. Strunnikov.

For observation of collapsed spindles, Smc3-GFP cells were treated with 20 μg/ml nocodozole in DMSO for 2–3 hr prior. Control cells were incubated in DMSO alone. Linescans were drawn through the fluorescence in cells treated with nocodazole versus untreated cells.

Hydroxyurea Arrest

Strains grown to early logarithmic phase were treated with 0.1M hydroxyurea (SIGMA). After 2–3 hr, more than 90% of cells were arrested with large buds. Temperature-sensitive *nuf2-45* or *ndc10-1* strains were grown to early logarithmic phase at 25°C and shifted to 37°C for 2–3 hr.

Alpha-Factor Arrest

Strains grown to early logarithmic growth phase were treated with 12 μg/ml of αF for 2–3 hr.

Fluorescence Microscopy

Image acquisition and fluorescence analysis were as previously described [S1]. Cells were immobilized onto ConA (SIGMA) coated coverslips, and 20 plane Z sections were acquired at 100 nm intervals through the cell with a Nikon 100× Plan-apochromat oil-immersion lens (Garden City, New York) on a spinning-disk confocal fluorescence microscope [S1]. The molecular count for Smc3p was obtained with a comparative fluorescence-signal measurement method similar to the one described in Joglekar et al. [S1]. Z sections of preanaphase cells expressing Smc3p-GFP and Spc29p-mRFP (KBY1983) were obtained with 200 nm spacing between successive images for the GFP channel and 500 nm spacing for the RFP channel. The spindle-pole positions were used to ensure that the spindle axis lies in the image plane. An 8 × 6 pixel (1064 × 798 nm) rectangle was manually placed around the Smc3p-GFP lobes in the plane that yielded the maximum integrated signal intensity. Background fluorescence subtracted from this integrated value was based on the average fluorescence signal in a nuclear region off the spindle axis. For conversion of the fluorescence signal into a molecular count, Cse4p-GFP (KBY7006) fluorescence signal was obtained from late anaphase or telophase cells under identical imaging conditions. Although this comparative method accounts for a different intensity distribution in the image plane, it assumes that the thickness of the Smc3p-GFP intensity distribution is diffraction limited. This assumption will result in a slight underestimation of the actual number of molecules.

The change in Smc3-GFP fluorescence as cells progress from metaphase to anaphase was quantitated according to the method described by Hoffman et al. [S2]. Live-cell images were obtained from cells immobilized on 25% gelatin/media slabs. Five plane Z sections at 200 nm steps through the cell were acquired at 1 min intervals. The microscope used for wide-field imaging was a Nikon Eclipse TE2000E stand (Nikon, Melville, New York) with 100 PlanApo NA 1.4 objective with a Hamamatsu Orca ER camera (Hamamatsu, Bridgewater, New Jersey). Images were acquired at room temperature with MetaMorph imaging software (Molecular Devices, Downingtown, Pennsylvania). In brief, a computer-generated 5 × 5 and 6 × 6 pixel regions were centered over the region of interest, and the total integrated fluorescence counts were obtained for each region. Inner- and outer-region data were transferred into Microsoft Excel (Microsoft, Richmond, Washington) with the use of the MetaMorph Dynamic Data Exchange function. The measured value for the 5 × 5 pixel region includes both cohesin fluorescence and local background fluorescence. The background component was obtained by subtraction of the integrated value of the 5 × 5 pixel region from the larger 6 × 6 pixel region. This result was scaled in proportion to the smaller area of the 5 × 5 pixel region and then subtracted from the integrated value of the 5 × 5 pixel region to yield a value for cohesin fluorescence.

3C Assay for Organization of Pericentric Chromatin

Yeast nuclei were prepared and crosslinked with 1% formaldehyde for 10 min at room temperature, with the goal of crosslinking any regions of the genome that were in physical proximity to one another. The reaction was quenched with the addition of glycine to 0.25 M. Nuclei were washed and resuspended in appropriate 1× restriction digest buffer. One percent SDS was added, and the nuclei were incubated at 65°C for 10 min to remove uncrosslinked proteins. Triton X-100 was added to a final concentration of 1% to remove the SDS and allow for subsequent digestion. Sixty units of the restriction enzyme XbaI were added, and the reaction was incubated overnight at 37°C. Ten percent SDS was added to each tube and incubated at 65°C for 20 min to inactivate XbaI. Eight hundred Weiss Units of T4 DNA ligase were added, and the reaction was incubated at 16°C for 2 hr to ligate crosslinked DNA. Crosslinks were then reversed with the addition of proteinase K and overnight incubation at 65°C. DNA was purified by phenol-chloroform extraction and ethanol precipitation. DNA concentration was determined by running of 1% agarose gels and staining with ethidium bromide. All gels were imaged with an Alpha Innotech Alphalmager 2200 imaging system, and all images were imported into Metamorph 6.1 for analysis. Gels were analyzed by measurement of the integrated intensity of a band and correcting for background as described in Joglekar et al. [S1]. Computer-generated boxes 5 × 5 and 6 × 6 pixel regions were centered over

each band, and the total integrated fluorescence counts were obtained for each region. The measured value for the 5 × 5 pixel region includes both product fluorescence and local background fluorescence. The background component was obtained by subtraction of the integrated value of the 5 × 5 pixel region from the larger 6 × 6 pixel region. This result was scaled in proportion to the smaller area of the 5 × 5 pixel region and then subtracted from the integrated value of the 5 × 5 pixel region to yield a value for product fluorescence. This method controls for inhomogeneity in background fluorescence.

Titration PCRs were performed with increasing amounts of input DNA. Input-DNA volumes that yielded PCR products that were within the linear range of PCR amplification were then used for 3C analysis. The crosslinking frequency of two ~15 kb regions of chromosome III were compared. One region, 15015 base pairs in length, spanned the centromere, bordered on either side by XbaI cut sites, one site being 6036 base pairs upstream of CEN3 and the other 8863 base pairs downstream of CEN3. The other region, 15835 base pairs in length, was located approximately 75 kb upstream of CEN3, with one XbaI cut site 23159 base pairs upstream and the other 38994 base pairs upstream. Ligation products from these regions are detected by PCR, yielding products approximately 500–700 base pairs in size. Nonspecific PCR products were not generated in any of the experiments. PCR products from crosslinked DNA were compared to identical products generated from control DNA, which was not crosslinked, allowing all possible ligation products to occur. Analysis of the resultant PCR products showed an average 56% increase in PCR product for the pericentric region as compared to the region along the arm, indicating a statistically significant increase in physical interaction of the genome at pericentric chromatin.

Supplemental References

S1. Joglekar, A.P., Bouck, D.C., Molk, J.N., Bloom, K.S., and Salmon, E.D. (2006). Molecular architecture of a kinetochore-microtubule attachment site. Nat. Cell Biol. *8*, 581–585.

S2. Hoffman, D.B., Pearson, C.G., Yen, T.J., Howell, B.J., and Salmon, E.D. (2001). Microtubule-dependent changes in assembly of microtubule motor proteins and mitotic spindle checkpoint proteins at PtK1 kinetochores. Mol. Biol. Cell *12*, 1995–2009.

S3. Winey, M., Mamay, C.L., O'Toole, E.T., Mastronarde, D.N., Giddings, T.H., Jr., McDonald, K.L., and McIntosh, J.R. (1995). Three-dimensional ultrastructural analysis of the Saccharomyces cerevisiae mitotic spindle. J. Cell Biol. *129*, 1601–1615.

S4. Dekker, J., Rippe, K., Dekker, M., and Kleckner, N. (2002). Capturing chromosome conformation. Science *295*, 1306–1311.

A

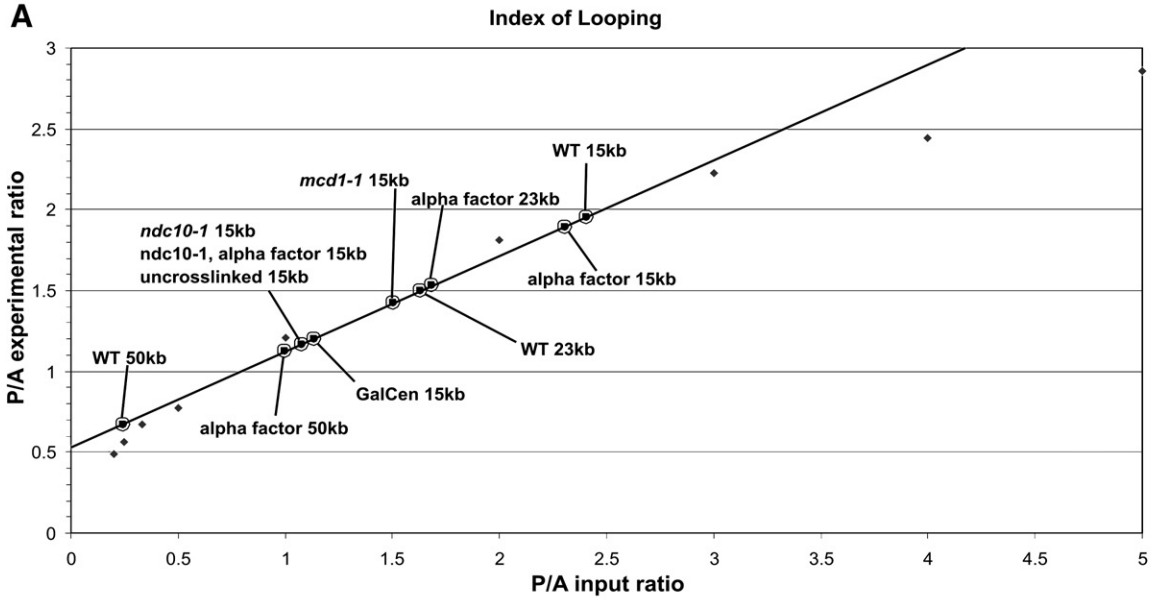

Picograms of input DNA	P	66	33	22	16.5	13.2	11	9.4	8.25	6.6
A	Fluor. Intensity	55799.45	37606.81	35540.79	28978.31	24298.12	21370.80	21434.12	18800.44	16510.35
66	49898.79	**1.12**	0.75	0.71	0.58	0.49	0.43	0.43	0.38	0.33
33	34056.65	1.64	**1.10**	1.04	0.85	0.71	0.63	0.63	0.55	0.48
22	28737.56	1.94	1.31	**1.24**	1.01	0.85	0.74	0.75	0.65	0.57
16.5	25505.52	2.19	1.47	1.39	**1.14**	0.95	0.84	0.84	0.74	0.65
13.2	20877.54	2.67	1.80	1.70	1.39	**1.16**	1.02	1.03	0.90	0.79
11	18548.31	3.01	2.03	1.92	1.56	1.31	**1.15**	1.16	1.01	0.89
9.4	16106.69	3.46	2.33	2.21	1.80	1.51	1.33	**1.33**	1.17	1.03
8.25	13873.03	4.02	2.71	2.56	2.09	1.75	1.54	1.55	**1.36**	1.19
6.6	12329.14	4.53	3.05	2.88	2.35	1.97	1.73	1.74	1.52	**1.34**

B

P/A product ratio	Crosslinked DNA	Uncrosslinked DNA	xlinked-unxlinked / unxlinked	Sample gel: P xlinked	A xlinked	P unxlinked	A unxlinked	n	P value
WT 15kb	1.96 ± .18	1.25 ± .15	56.46%					10	4.46E-08
WT 23kb	1.28 ± .05	1.04 ± .03	23.81%					5	1.02E-05
WT 50kb	1.22 ± .25	2.16 ± .30	-43.81%					5	2.82E-04
αF 15kb	1.90 ± .21	1.22 ± .07	56.02%					10	1.33E-08
αF 23kb	1.26 ± .03	1.00 ± .03	25.91%					5	6.37E-07
αF 50kb	1.74 ± .05	1.87 ± .04	-6.58%					5	.002
ndc10-1 15kb	1.21 ± .08	1.18 ± .09	2.03%					10	.55
ndc10-1, αF 15kb	1.21 ± .03	1.20 ± .02	1.56%					10	.76
mcd1-1 15kb	1.44 ± .14	1.18 ± .05	22.17%					10	3.89E-05
gal cen 15kb	0.63 ± .05	0.62 ± .06	1.76%					10	.67

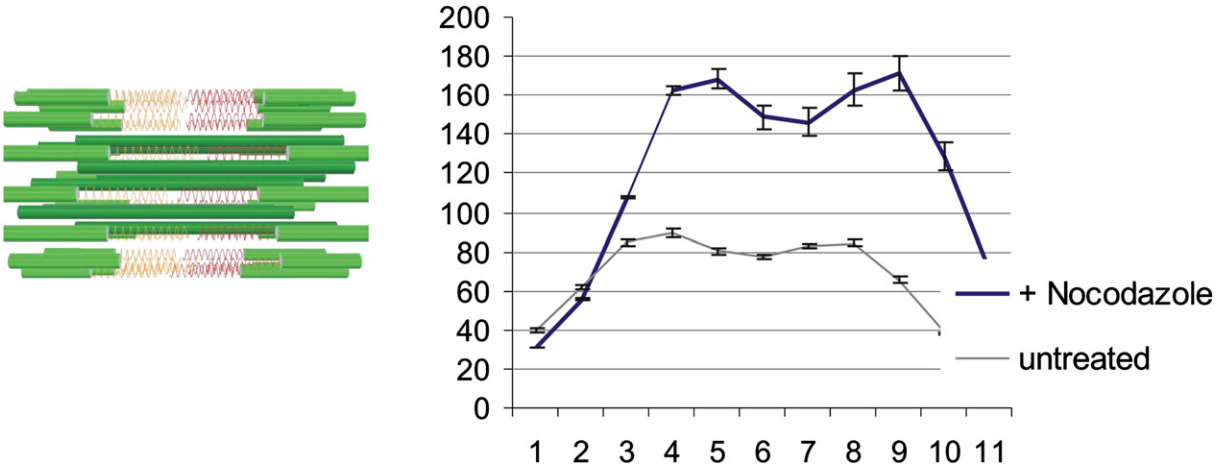

Figure S4. Distribution of Cohesin upon Nocodazole Treatment

Distribution of Smc3-GFP in nocodazole-treated cells. Left: A schematic of a collapsed spindle in sagittal view. The height of the cylinder is decreased as a consequence of spindle-pole collapse. Right: Linescans of untreated versus treated (+ nocodazole) fluorescent images. Linescans are perpendicular to the spindle axis [vertical on the schematic; x axis, arbitrary fluorescence units; y axis, pixels (65 nm/pixel)]. Note the increase of fluorescence per pixel in the nocodazole-treated relative to untreated. Error bars are standard error of the mean (average of 24 cells).

Figure S3. Conversion of 3C PCR Data to Looping Index

(A) Standard curve for the chromosome-capture technique 3C [S4]. A standard curve was generated by performing PCR reactions with known quantities of reconstructed template spanning the experimental intramolecular crosslinking sites. Template for PCR reaction with pericentric primer pairs (P_{1u}, P_{1d}, see Figure 5A) was built by amplifying two fragments, extending from the position of oligonucleotides P_{1u}, P_{1D} shown in Figure 5A to the XbaI sites (P_{1u} to XbaI 191 bp fragment; P_{1D} to XbaI 277 bp fragment; XbaI 108347; p_1 oligonucleotide, 108538–108564; *CEN3*, 114383–114499; P_{1D}, 123083–123109; XbaI, 123360). The 191 bp P_{1u} to *XbaI* fragment and 277 bp P_{1D} to XbaI fragments were amplified and cut with XbaI. Ligation of these two products generates the template representing the intramolecular loop in the experimental pericentric sample. The template for PCR reaction with arm primer pairs (A_u + A_d) was built by amplification of two fragments, extending from the position of oligonucleotides A_U + A_D shown in Figure 5A to the respective XbaI sites (A_D to XbaI 251 bp fragment; A_U to XbaI 220 bp fragment; XbaI, 23160; A_D oligonucleotide, 23383–23410; A_U oligonucleotide 38744–38770; XbaI, 38994). The 251 bp A_D to XbaI fragment and 220 bp A_U to XbaI were amplified and cut with XbaI. Ligation of the two products generates the template representing the intramolecular loop in the experimental arm sample. The concentration of each ligation product was determined by optical density and PCR reactions with templates of known concentration were performed. PCR conditions were as described for the experimental sample. The products were analyzed by gel electrophoresis, and product intensity was determined as described in the Experimental Procedures. The raw fluorescence-intensity values for each product at a given concentration of input template are indicated in the table below the graph. The graph is a standard curve from reactions with reconstructed input P:A templates (P:A input ratio, x axis) versus reactions with experimental templates (P:A experimental ratio, y axis). The value for the experimental P:A ratio of 1.0 was calculated from the experimental fluorescence intensity from average of all the input pericentric (P) template concentrations of 66 pg to 6.6 pg divided by all the input arm (A) template concentrations of 66 pg to 6.6 pg (shown in bold) (1.12 + 1.1 + 1.24 + 1.14 + 1.16 + 1.15 + 1.33 + 1.36 + 1.34) = 1.21. At an equal concentration of pericentric and arm templates, the experimental ratio of P:A product is 1.21. The P:A input ratios were calculated from the data in the graph for P:A ratios of 0.2 to 5.0 and are plotted above (black diamonds). The experimental reactions were performed over the linear range of this plot (0.3–2.5). The looping index (x axis) is a method to normalize the experimental product yield to the actual input product.

(B) Experimental samples (wild-type [WT], *ndc10-1*, αF-treated cells, *mcd1-1*, and GALCEN). Samples from each experimental treatment were prepared as described in the Experimental Procedures. Representative PCR products from each experiment are shown (n = 5 or 10 number of independent determinations). The amount of product was in the linear range of PCR reactions shown in (A). The P:A ratio was determined by division of the fluorescence intensity (or picograms) of pericentric PCR product by the fluorescence intensity (or picograms) of arm product. Samples were prepared from crosslinked and uncrosslinked treatments. In uncrosslinked samples, the P:A ratio (1.2) reflects an equal concentration of P:A input template (A). In crosslinked samples, the P:A ratio reflects the change in product formation (increased or decreased) relative to uncrosslinked. The change in the crosslinked versus uncrosslinked treatments is shown as the % change relative to uncrosslinked ((crosslinked − uncrosslinked) / uncrosslinked). For the looping index (A), the crosslinked P:A experimental ratio values are plotted on the y axis to determine the actual change in concentration of input product in the different samples.

Table S1. Molecular Counting of Smc3-GFP

	Signal	Ratio	# of Molecules
Smc3-GFP[a] (cylinder)	5110 ± 2060	3.37	108 ± 43
Cse4-GFP	1515 ± 213		
Smc3-GFP[b] (whole cell, confocal)	14534 ± 3562	20	638 ± 156
Cse4-GFP (whole cell, confocal)	728 ± 437		
Smc3-GFP[c] Nocodazole	11413 ± 6295	6.95	222 ± 122
Cse4-GFP Nocodazole	1640 ± 240		

[a] For cylinder measurements, the size of the measurement rectangle was based on the dimensions of the cylinder reported in the paper.

[b] For whole-cell measurements, three strains were mixed together—473a, Cse4-GFP, and Smc3-GFP. Eleven planes spaced 600 nm apart were taken in each field on the spinning-disk confocal microscope. For fluorescence quantification, the 11 planes were summed together. Only preanaphase cells were selected for the analysis. An elliptical region of interest was drawn to include majority of the mother cell as seen in the transmitted light image. Fluorescence signal from this region was integrated and considered as the signal from the GFP-tagged protein. The 473a cells provided the average background fluorescence per pixel, which was subtracted from the measured signals for Cse4-GFP and Smc3-GFP before they were compared.

[c] Cells expressing Smc3-GFP and Spc29-mRFP were treated with 20 μg/ml nocodazole for 2 hr at 32°C. For evaluation of the fluorescence intensity, linescans from GFP fluorescence spots colocalizing with the SPBs were fitted with 1D Gaussian functions to determine the spatial extent of fluorescence intensity distribution so that the number of pixels to be integrated could be deteremined (11 pixels on average with 1 pixel ~133 nm). A Z stack of images with 200 nm spacing was obtained for each cell, and the plane of maximum signal value in the region of interest was selected for the quantification.